ACCEPTED MANUSCRIPT

PLEASE CITE THIS ARTICLE AS DOI: 10.1063/5.0033236

Journal of Applied Physics

AIP Publishing

Interface-driven magnetic anisotropy in relaxed $La_{0.7}Sr_{0.3}CrO_3/La_{0.7}Sr_{0.3}MnO_3$ heterostructures on MgO

Sanaz Koohfar,[1] Yasemin Ozbek,[1] Hayden Bland,[1] Zhan Zhang,[2] and Divine P. Kumah[1, a)]

[1)] *Department of Physics, North Carolina State University, Raleigh, NC 27695, USA*

[2)] *Advanced Photon Source, Lemont, IL 76019, USA*

We investigate the structural and magnetic properties of $La_{0.7}Sr_{0.3}CrO_3$ (LSCO)/$La_{0.7}Sr_{0.3}MnO_3$(LSMO) heterostructures grown on (001)-oriented MgO by molecular beam epitaxy. Due to the large film-substrate lattice mismatch, strain relaxation is found to occur within the first 2-3 unit cells (uc) of the film as evidenced by reflection high energy electron diffraction and high-resolution synchrotron X-ray reciprocal space mapping. We find that the presence of the LSCO spacer and capping layers leads to ferromagnetism in ultra-thin LSMO layers with thicknesses on the order of 2 uc with the magnetic easy axis oriented in the film plane. Net magnetic moments of 1.4 and 2.4 μ_B/Mn are measured for [2 uc LSCO/ 2 uc LSMO] and [2 uc LSCO/ 4 uc LSMO] superlattices, respectively by SQUID magnetometry. The effective magnetic anisotropy of the relaxed [2 uc LSCO/ 4 uc LSMO] heterostructure is found to be an order of magnitude higher than bulk LSMO highlighting the critical role of interfacial interactions in tuning magnetic anisotropy at complex oxide interfaces.

[a)]Electronic mail: Author to whom correspondence should be addressed: dpkumah@ncsu.edu

ACCEPTED MANUSCRIPT

PLEASE CITE THIS ARTICLE AS DOI: 10.1063/5.0033236

Journal of Applied Physics

AIP Publishing

I. INTRODUCTION

Doped rare-earth manganites ($A_{1-x}B_xMnO_3$ where A is a rare-earth ion and B is an alkaline-earth ion) exhibit a wide range of interesting physical properties including tunable magnetic phases and metal-insulator transitions, colossal magnetoresitivity and half metallicity.[1,2] For bulk $La_{1-x}Sr_xMnO_3$ (LSMO) with 30% Sr doping, a ferromagnetic metallic state exists below 360 K.[3,4] Due to the strong coupling of the lattice, spin and electronic degrees of freedom, the transport and magnetic properties of LSMO thin films have been tuned by epitaxial growth on closely lattice-matched single crystal substrates such as $LaAlO_3$, $SrTiO_3$, $DyScO_3$ and LSAT.[5–7] Epitaxial strain provides an effective route to control magnetic anisotropy in LSMO thin films with important implications for the design of novel spin-based devices.[8–11] The magnetic easy axis for LSMO films under tensile strain on $SrTiO_3$ lies in-plane along the [110] pseudocubic axis while compressively strained films on $LaAlO_3$ exhibit strong perpendicular magnetic anisotropy.[8] As the film thickness is reduced to the dimensions on the order of a unit cell, surface and interfacial contributions to magnetic anisotropy energy are non-negligible and compete with strain-mediated contributions to magnetocrystalline anisotropy.[12,13]

An interface-induced magnetic anisotropy has been reported for $SrIrO_3/La_{1-x}Sr_xMnO_3$ superlattices where an increase in the perpendicular magnetic anisotropy (PMA) is correlated with an increase in oxygen octahedral rotations about an in-plane axis as a function of the Sr content.[14] A PMA has also been reported for tensile-strained $La_{1-x}Sr_xCoO_3/La_{1-x}Sr_xMnO_3$ bilayers For the relaxed LSCO/LSMO heterostructures, the in-plane and out-of-plane rotations are expected to be bulk-like and equivalent along the orthogonal pseudo-cubic axes. Recent results indicate that an interface-induced preferential occupations of the Mn 3d orbitals can result in spin-reorientation transitions. Song *et. al.* show that an interplay between ferromagnetic interfacial Mn-O-Co exchange, charge transfer and a preferential occupation of out-of-plane pointing Mn 3d $z^2 - r^2$ orbitals are associated with a PMA in tensiley strained $LaSrCoO_3/LaSrMnO_3$ bilayers.[13] By tuning Co-Mn charge transfer and the interfacial orbital polarization via ionic-liquid gating, a reorientation of the magnetic easy axis in the in-plane direction is achieved. Additional reports on compressively strained $LaSrCoO_3/LSMO/LSrCoO_3$ trilayers show an in-plane easy axis in contrast to a PMA observed for single layer compressively strained LSMO on $LaAlO_3$ due to off-center Mn

ACCEPTED MANUSCRIPT

PLEASE CITE THIS ARTICLE AS DOI: 10.1063/5.0033236

Journal of Applied Physics

AIP Publishing

displacements which favor a preferential occupation of the in-plane Mn 3d $x^2 - y^2$ orbitals.[15]

For uncapped stoichiometric LSMO films, below a critical thickness of 4-10 nm, ferromagnetism is suppressed limiting potential applications in thin film devices and a direct decoupling of the various contributions to magnetic anisotropy.[5,16] The suppression of ferromagnetism in thin LSMO films has been attributed to structural distortions and chemical and electronic reconstructions arising from interfacial polar discontinuities,[17–20], oxygen vacancies[21], cation disorder[22], orbital reconstructions[23] and distortions of the oxygen octahedra due to interfacial structural coupling.[24–27] Recent reports on coherently strained LSMO layers in LSMO/$SrRuO_3$ superlattices[28] and LSMO layers capped with $La_{0.7}Sr_{0.3}CrO_3$ (LSCO) have evidenced ferromagnetism in LSMO layers as thin as 2 unit cells (0.8 nm).[6,29–31]

In this letter, we investigate the structural and magnetic properties of strain-free LSCO/LSMO heterostructures grown on (001)-oriented single crystal MgO substrates.[32–34] Bulk LSMO and LSCO have pseudocubic lattice constants of 3.88 and 3.86 Å respectively. The lattice mismatch of LSMO and LSCO with cubic MgO (c=4.212 Å) is 8.5%. Due to the large tensile lattice mismatch between the MgO substrate and the LSMO and LSCO layers, strain relaxation is found to occur within the first 2-3 unit cells of the film as evidenced by *in-situ* reflection high energy electron diffraction measurements and *ex-situ* X-ray diffraction. A paramagnetic-ferromagnetic transition is observed for heterostructures with 2 unit cell (u.c.) thick LSMO layers indicative of the removal of magnetically dead LSMO layers. The relaxed states of the ultra-thin LSMO films allows us to elucidate the role of confinement to magnetic anisotropy in this system. The magnetic easy axis is found to lie in the plane of the film due to the dominant contributions of LSCO/LSMO interfacial interactions and confinement to the total magnetic anisotropy.

II. EXPERIMENTAL PROCEDURE

Trilayer 3 uc LSCO/ 3 uc LSMO/ 3uc LSCO films (referred to as (3/3/3)) and [2 uc LSCO/N uc LSMO]$_x$ superlattices (where x is the number of repeats) were fabricated by molecular beam epitaxy (MBE) on (001)-oriented MgO substrates. The LSMO layer thickness, N, was varied from 2-6 ucs and the superlattices were capped with 2 uc LSCO. Prior to growth, the MgO substrates were etched in buffered hydrofluoric acid and annealed in a tube furnace at 1200 ^{o}C to achieve atomically flat surfaces. The films were grown at a substrate

ACCEPTED MANUSCRIPT

PLEASE CITE THIS ARTICLE AS DOI: 10.1063/5.0033236

Journal of Applied Physics

AIP Publishing

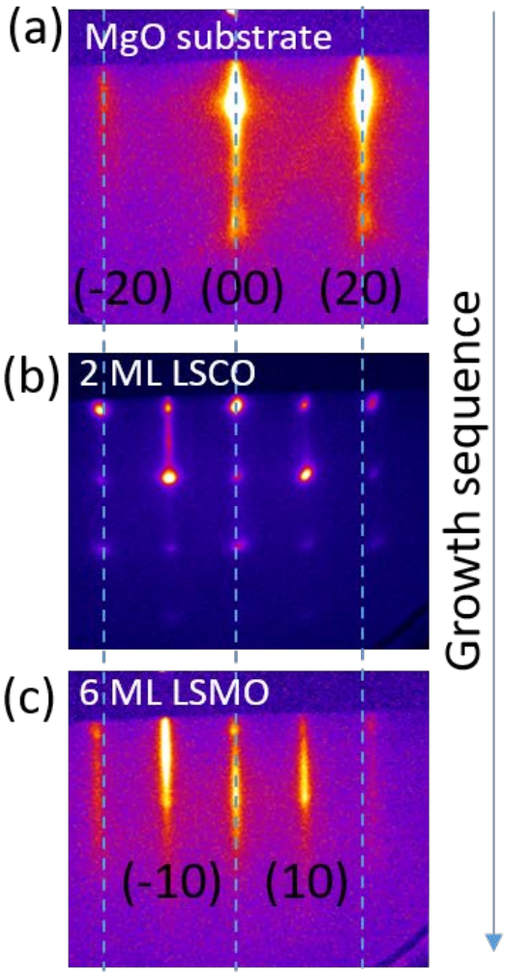

FIG. 1. Reflection high energy diffraction (RHEED) pattern recorded along high symmetry zone axes during the growth of a 2 uc LSCO/6 uc LSMO bilayer for (a) the initial MgO substrate (b) the first 2 uc of LSCO indicating 3D growth and for (c) 6 uc of LSMO indicating a transition to 2D growth. The shift of the (2 0) diffraction pattern of the film is indicative of a contraction of the in-plane lattice constant from 4.21 Å for the MgO substrate to $\sim$ 3.87 Å for the LSCO and LSMO layers. The vertical dashed lines indicate the position of the MgO (2 0) reflection.

temperature determined by an optical pyrometer of 850 $\pm$25 ^{o}C using an oxygen plasma source with an oxygen partial pressure of 3x10^{-6} Torr. After growth, the films were cooled to room temperature at a rate of 5 ^{o}C/min at the growth oxygen pressure to minimize the formation of oxygen vacancies. *In-situ* reflection high energy electron diffraction (RHEED) was used to monitor the film thickness and crystallinity during growth.

ACCEPTED MANUSCRIPT

PLEASE CITE THIS ARTICLE AS DOI: 10.1063/5.0033236

Journal of Applied Physics

AIP Publishing

To determine the strain states of the samples, reciprocal space maps of the 3/3/3 trilayer sample were measured at room temperature the 33ID beamline at the Advanced Photon Source with a Pilatus 100K pixel detector.[35] Specular diffraction scans of the film and substrate Bragg peaks for the [2 LSCO/4 LSMO]$_6$ and [2 LSCO/6 LSMO]$_4$ superlattices were measured using a Rigaku Smartlab diffractometer equipped with a Ge(220) double bounce monochromator.

Temperature and magnetic field-dependent measurements of the magnetization of the samples were performed by superconducting quantum interference device (SQUID) magnetometry using a Quantum Design MPMS 3 system. The temperature-dependent magnetization curves were measured on warming up the sample with an applied 0.1 T magnetic field after field cooling in an 1 T magnetic field. The magnetization measurements were performed with the applied magnetic field oriented either parallel to the film [100] axis (in-plane) or to the film [001] axis (out-of-plane).

III. RESULTS AND DISCUSSION

A. X-ray diffraction measurements

The evolution of the RHEED pattern during the growth of the first LSCO and LSMO layers is shown in Fig. 1. A transition in the RHEED spectra from the diffraction pattern for the MgO substrate surface in Fig. 1(a) to 3D spots (Fig. 1(b)) after deposition of 2 uc of LSCO is indicative of initial island growth and surface roughening. Additionally, an increase in the spacing of the RHEED streaks indicates a decrease in the in-plane lattice constant from 4.21 Å for the MgO surface to ∼3.87 ±0.02 Å for the LSCO adlayer. On deposition of 6 uc of LSMO, the RHEED pattern transitions from the 3D pattern to 2D streaks shown in Fig. 1(c) indicative of a smoothening of the film surface. The initial roughening is attributed to a 3D Volmer-Weber island growth to relax the large film-substrate lattice mismatch.[36]

To confirm the relaxation of strain in the LSCO/LSMO layers, reciprocal space maps were measured at the 33ID beamline at the Advanced Photon Source with an incident photon energy of 15.5 keV. Fig. 2 shows the reciprocal space map around the LSCO/LSMO film (111) and the MgO (111) Bragg peak for a trilayer 3 uc LSCO/ 3uc LSMO/ 3uc LSCO sample on MgO. The location of the film Bragg peak corresponds to a relaxed pseudo-cubic

ACCEPTED MANUSCRIPT

PLEASE CITE THIS ARTICLE AS DOI: 10.1063/5.0033236

Journal of Applied Physics

AIP Publishing

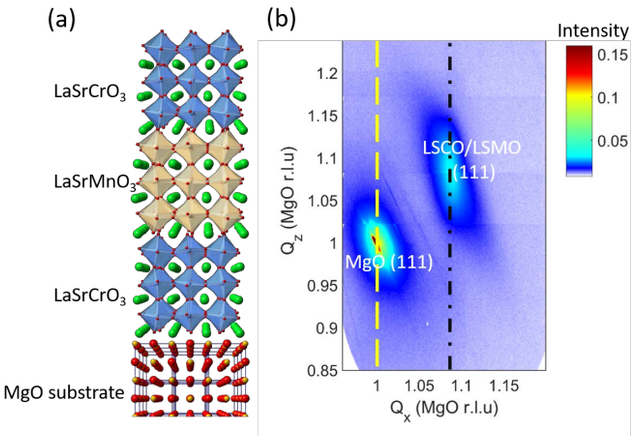

FIG. 2. (a) Schematic of 3 uc $LaSrCrO_3$/ 3 uc $LaSrMnO_3$/ 3 uc $LaSrCrO_3$ heterostructure grown on (001)-oriented MgO by molecular beam epitaxy. (b) The reciprocal space map around the film and substrate (111) Bragg peaks indicate film strain relaxation. The yellow and black vertical dashed lines indicate the in-plane reciprocal vector corresponding to bulk MgO and LSMO respectively.

lattice constant of a=b=c=3.87 ± 0.01 Å.

The out-of-plane lattice constants of the superlattices are determined from specular diffraction scans around the film and substrate (002) Bragg peaks. The (002) Bragg peaks for $[2$ uc LSCO/4 uc LSMO$]_6$ and $[2$ uc LSCO/6 uc LSMO$]_4$ superlattices on MgO substrates are shown in Fig. 3. The fits to the measured data are obtained using the GenX X-ray analysis program.[37] The average out-of-plane lattice constant determined from the fits for the LSMO and LSCO layers are 3.868±0.005 and 3.862±0.005 Å respectively. The calculated lattice parameters obtain from the fit is very close to the bulk LSMO lattice constant which further supports the lattice relaxation in LSCO/LSMO heterostructures on MgO.[38]

B. Magnetization measurements

To determine the effect of the lattice relaxation on the magnetic properties of the heterostructures, magnetization as a function of applied magnetic field and temperature were measured by SQUID magnetometry. The temperature-dependent curves were measured with a 1000 Oe magnetic field applied either in-plane or out-of-plane on warming after field cooling in a 1 T applied magnetic field. The magnetization as a function of magnetic field and temperature for the $[2$ LSCO/2 LSMO$]_{10}$ and $[2$ LSCO/4 LSMO$]_6$ superlattices on MgO

ACCEPTED MANUSCRIPT

PLEASE CITE THIS ARTICLE AS DOI: 10.1063/5.0033236

Journal of Applied Physics

AIP Publishing

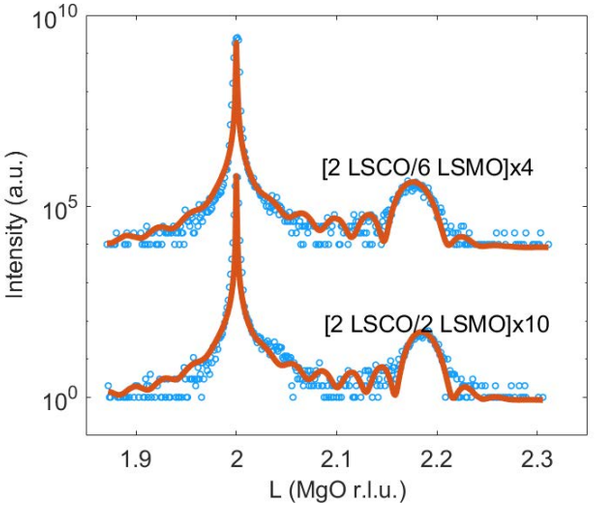

FIG. 3. Measured (circles) and simulated (solid lines) specular diffraction of $[2\ \mathrm{LSCO}/2\ \mathrm{LSMO}]_{10}$ superlattice and $[2\ \mathrm{LSCO}/6\ \mathrm{LSMO}]_4$ superlattice on MgO substrate. The diffraction spectra are offset for clarity. L is the reciprocal lattice unit of the MgO substrate where 1 r.l.u.=$(1/4.212)\text{Å}^{-1}$.

are shown in Fig. 4(a) and Fig. 4(b), respectively with the magnetic field oriented either in-plane or out-of plane as shown in the inset in Fig. 4(a). For both samples, the magnetization is significantly reduced in the out-of-plane direction compared to the in-plane magnetization indicative of an in-plane magnetic easy axis. For the $[2\ \mathrm{LSCO}/2\ \mathrm{LSMO}]_{10}$ sample, the out-of-plane magnetization does not reach the saturation value measured for the in-plane orientation.

Furthermore, the observation of of ferromagnetism in the heterostructure with LSMO thickness of 2 uc is attributed to the removal of magnetic dead layers when using LSCO as spacer due to the interfacial structural coupling and the anti-ferromagnetic coupling between Cr and Mn across the LSCO/LSMO interface.[6] The measured magnetic moments for the relaxed heterostructures on LSMO are expected to be close or identical to analogous heterostructures grown on LSAT where the lattice mismatch is small (0.2%).[29] The magnetic moments for the $[2\ \mathrm{LSCO}/2\ \mathrm{LSMO}]_{10}$ and $[2\ \mathrm{LSCO}/4\ \mathrm{LSMO}]_6$ heterostructures on LSAT at 10 K are 1.5 μ_B/Mn and 2.8 μ_B/Mn respectively. The corresponding moments for the $[2\ \mathrm{LSCO}/2\ \mathrm{LSMO}]_{10}$ and $[2\ \mathrm{LSCO}/4\ \mathrm{LSMO}]_6$ on MgO are 1.4 and 2.4 μ_B/Mn respectively. The increase in the magnetization per Mn with increasing LSMO thickness is attributed to the contribution to the total magnetization of the Cr spins aligned anti-parallel to the

ACCEPTED MANUSCRIPT

PLEASE CITE THIS ARTICLE AS DOI: 10.1063/5.0033236

Journal of Applied Physics

AIP Publishing

applied magnetic field.[6,29]

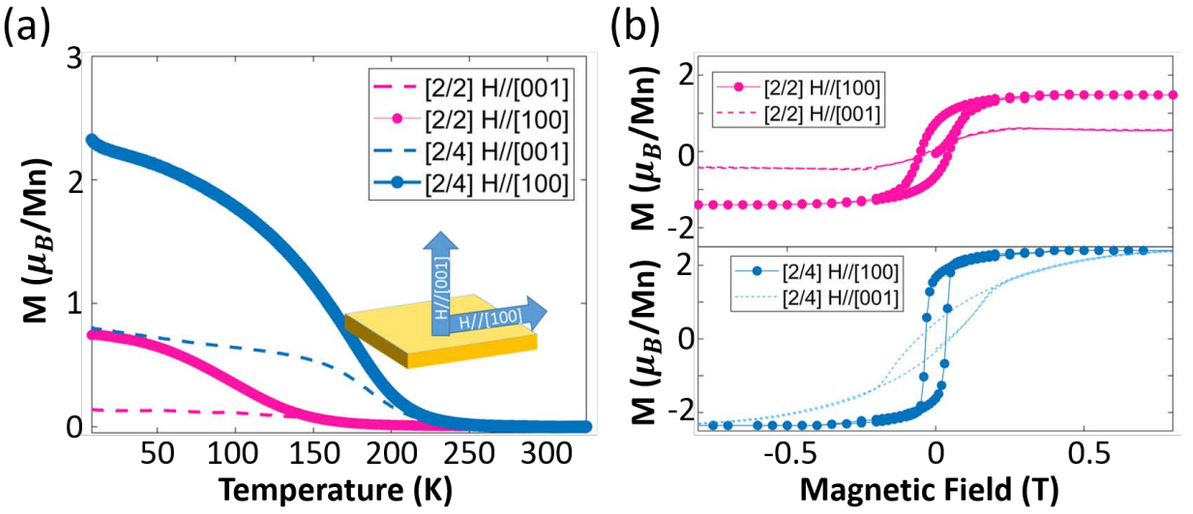

FIG. 4. (a) Temperature-dependent in-plane and out-of-plane magnetization measurements with 1000 Oe applied field on warming after a 0.5 T field cooling in a 1 T field. and (b) Field-dependent magnetization curves at 10 K for [2 LSCO/ 2 LSMO]$_{10}$ and [2 LSCO/ 4 LSMO]$_6$ superlattices grown on (001)-oriented MgO by molecular beam epitaxy.

To quantify the magnetic anisotropy (MA) between the magnetic easy and hard axis, we calculate the magnitude of the effective anisotropy constant, K_{eff}, by the area enclosed between the in-plane, M_{ip}, and out-of-plane, M_{oop}, magnetization curves shown in Fig. 4(b) for the [2 LSCO/4 LSMO]$_6$ heterostructure.[39,40] K_{eff} for the [2 LSCO/4 LSMO]$_6$ configuration is approximately -2$\times$10^5 ergs/cm^3 which is comparable to that of strained LSMO.[8] The measured anisotropy for the relaxed heterostructure is unexpected since the magnetocrystalline anisotropy for bulk LSMO is 1 order of magnitude lower.[41]

For thin films, the effective anisotropy energy K_{eff} can be expressed in terms of a bulk magnetocrystalline contribution K_V and a surface/interface contribution K_S as[39]

$$K_{eff} = \mu_0 \int_0^{H_S} M_{oop} dH - \mu_0 \int_0^{H_S} M_{ip} dH = K_V + 2\pi M_S + \frac{K_S}{t_{FM}} \quad (1)$$

where K_V is the intrinsic bulk anisotropy and K_S/t_{FM} is the interface anisotropy due to the interfacial exchange bias and/or surface and interface induced structural and orbital reconstructions and t_{FM} is the thickness of the ferromagnetic LSMO layer.[15,23,42] The $2\pi M_S$

ACCEPTED MANUSCRIPT

PLEASE CITE THIS ARTICLE AS DOI: 10.1063/5.0033236

Journal of Applied Physics

AIP Publishing

term is the shape magnetic ansiotropy. A positive K_{eff} corresponds to a perpendicular magnetic anisotropy and $K_{eff} < 0$ corresponds to an in-plane easy axis.[39] Thus, the negative K_{eff} observed for the LSCO/LSMO heterostructures suggests that the interfacial contribution K_S/t_{FM} which depends on the film thickness is negative and its contribution to the total magnetic anisotropy will decrease with increasing t_{FM}. For the [2 LSCO/2 LSMO] heterostructure, the out-of-plane magnetization does not reach saturation magnetization observed for the measurements with the magnetic field oriented in-plane suggesting that K_{eff} is dominated by K_S. We note that the net magnetization measured by SQUID for the LSCO/LSMO heterostructures depends on the magnetization in both the Cr and Mn layers, thus, the effect of magnetic anisotropy on both the LSMO and LSCO layers determines the total magnetic response.[6,29] Further studies are required to determine how the orientation of the external field affects the interfacial magnetic exchange at the LSCO/LSMO interface.

To confirm that the easy in-plane axis observed for the relaxed LSCO/LSMO heterostructures on MgO is independent of strain, element-selective X-ray magnetic circular dichroism (XMCD) measurements are carried out as a function of an applied magnetic field for a $[2\ \text{LSMO}/2\ \text{LSCO}]_{10}$ superlattice under coherent 2% compressive strain on a $LaAlO_3$ substrate.[29] The XMCD measurements were performed at the 4.0.2 beamline at the Advanced Light Source using total electron yield with an incident beam angle at 30 degrees to the sample surface. The X-ray absorption spectra (XAS) at the Mn L-edge measured for right ($I(\sigma^+)$) and left ($I(\sigma^-)$) circular polarized incident photons with a 0.5 T magnetic field applied in the plane of the sample are compared in Figure 5(a). The XMCD signal is determined from the difference between $I(\sigma^+)$ and $I(\sigma^-)$. Furthermore, XMCD magnetic hysteresis loops are obtained by fixing the photon energy at the Mn L_3 edge and measuring the XMCD signal as the applied magnetic field is swept between -0.5 T and 0.5 T. We compare the XMCD hysteresis loops measured at the Mn L_3 absorption edge at 150 K for a magnetic field applied in-plane and out-of plane as shown in Figure 5(b). The XMCD results indicate an in-plane easy axis for the compressively strained LSCO/LSMO heterostructure, hence, the observed MA is attributed to interactions at the LSCO/LSMO interface which dominate the magnetocrystalline and shape anisotropy for ultra-thin LSMO layers.

ACCEPTED MANUSCRIPT

PLEASE CITE THIS ARTICLE AS DOI: 10.1063/5.0033236

Journal of Applied Physics

AIP Publishing

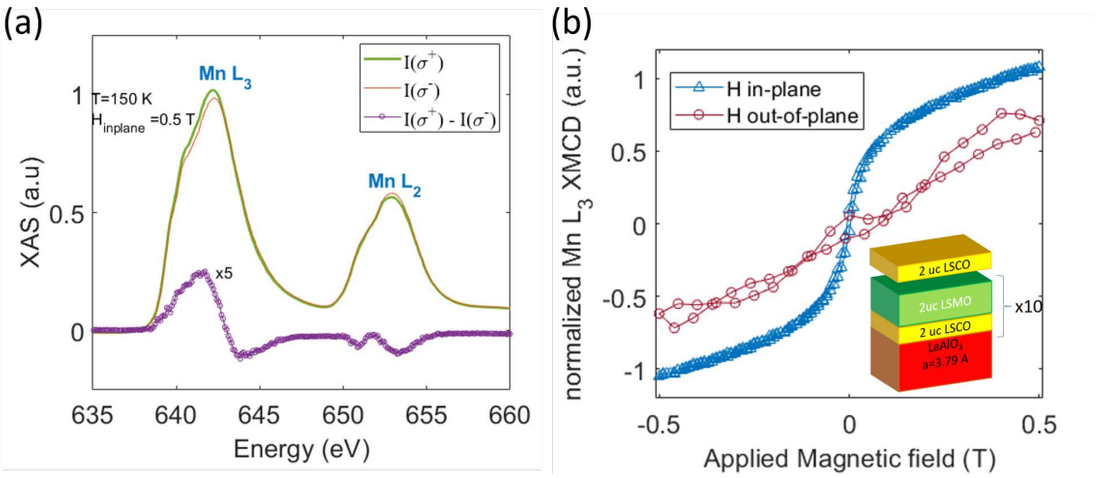

FIG. 5. (a) X-ray absorption spectra measured at the Mn L-edge for right ($I(\sigma^+)$) and left ($I(\sigma^-)$) circular photon polarization and the XMCD signal, $I(\sigma^+)$-$I(\sigma^-)$, for a $[2\ LSCO/\ 2\ LSMO]_{10}$ heterostructure on $LaAlO_3$. The measurements are performed at 150 K with a 0.5 T magnetic field applied in the plane of the sample. (b) Magnetic field dependence of the XMCD signal measured at the Mn L_3-edge and 150 K for a $[2\ LSCO/\ 2\ LSMO]_{10}$ /$LaAlO_3$ sample with the field applied either parallel or perpendicular to the film surface.

IV. CONCLUSION

In conclusion we have investigated the effect of LSCO spacer layers on the magnetic properties of thin LSMO layers grown on (001)-MgO substrates. The LSCO/LSMO heterostructures are found to be relaxed as a result of the large lattice mismatch with the MgO substrate with strain relaxation occurring within 2-3 unit cells. The magnetic easy axis of the LSCO/LSMO heterostructures is found to lie in the plane of the film due to a dominant contribution of the LSMO interface magnetic anisotropy to the total magnetic anisotropy. This work demonstrates the critical role interfacial interactions play in modulating the magnetic states of transition metal oxide heterostructures.

ACKNOWLEDGMENTS

S.K., Y.O. and D.P.K. acknowledge financial support by the US National Science Foundation under Grant No. NSF DMR-1751455. This work was performed in part at the

ACCEPTED MANUSCRIPT

PLEASE CITE THIS ARTICLE AS DOI: 10.1063/5.0033236

Journal of Applied Physics

AIP Publishing

Analytical Instrumentation Facility at North Carolina State University, which is supported by the State of North Carolina and the National Science Foundation (award number ECCS-1542015). This work made use of instrumentation at AIF acquired with support from the National Science Foundation (DMR-1726294). The AIF is a member of the North Carolina Research Triangle Nanotechnology Network (RTNN), a site in the National Nanotechnology Coordinated Infrastructure (NNCI). The authors acknowledge use of the SQUID and PPMS facility in the Department of Materials Science and Engineering at North Carolina State University. Use of the Advanced Photon Source was supported by the U.S. Department of Energy, Office of Science, Office of Basic Energy Sciences, under Contract No. DE-AC02-06CH11357.This research used resources of the Advanced Light Source, which is a DOE Office of Science User Facility under contract no. DE-AC02-05CH11231.

DATA AVAILABILITY

The data that support the findings of this study are available from the corresponding author upon reasonable request.

REFERENCES

[1]N. F. Mott, Advances in Physics **13**, 325 (1964).

[2]Y. Tokura, *Colossal magnetoresistive oxides* (CRC Press, 2000).

[3]S. Ikeda, K. Miura, H. Yamamoto, K. Mizunuma, H. Gan, M. Endo, S. Kanai, J. Hayakawa, F. Matsukura, and H. Ohno, Nature Materials **9**, 721 (2010).

[4]S. Mangin, D. Ravelosona, J. Katine, M. Carey, B. Terris, and E. E. Fullerton, Nature Materials **5**, 210 (2006).

[5]F. Tsui, M. Smoak, T. Nath, and C. Eom, Applied Physics Letters **76**, 2421 (2000).

[6]S. Koohfar, A. B. Georgescu, A. N. Penn, J. M. LeBeau, E. Arenholz, and D. P. Kumah, npj Quantum Materials **4**, 25 (2019).

[7]Y. Konishi, Z. Fang, M. Izumi, T. Manako, M. Kasai, H. Kuwahara, M. Kawasaki, K. Terakura, and Y. Tokura, Journal of the Physical Society of Japan **68**, 3790 (1999).

[8]Y. Suzuki, H. Hwang, S.-W. Cheong, and R. Van Dover, Applied Physics Letters **71**, 140 (1997).

ACCEPTED MANUSCRIPT

PLEASE CITE THIS ARTICLE AS DOI: 10.1063/5.0033236

Journal of Applied Physics

AIP Publishing

[9]L. Berndt, V. Balbarin, and Y. Suzuki, Applied Physics Letters **77**, 2903 (2000).

[10]H. Boschker, M. Mathews, E. P. Houwman, H. Nishikawa, A. Vailionis, G. Koster, G. Rijnders, and D. H. Blank, Physical Review B **79**, 214425 (2009).

[11]Z. Liao, M. Huijben, Z. Zhong, N. Gauquelin, S. Macke, R. J. Green, S. Van Aert, J. Verbeeck, G. Van Tendeloo, K. Held, G. A. Sawatzky, G. Koster, and G. Rijnders, Nature Materials **15**, 425 (2016).

[12]D. Yi, J. Liu, S.-L. Hsu, L. Zhang, Y. Choi, J.-W. Kim, Z. Chen, J. D. Clarkson, C. R. Serrao, E. Arenholz, P. J. Ryan, H. Xu, R. J. Birgeneau, and R. Ramesh, Proceedings of the National Academy of Sciences **113**, 6397 (2016).

[13]J. Song, Y. Chen, X. Chen, T. Khan, F. Han, J. Zhang, H. Huang, H. Zhang, W. Shi, S. Qi, F. Hu, B. Shen, and J. Sun, Physical Review Applied **14**, 024062 (2020).

[14]L. Wu, C. Li, M. Chen, Y. Zhang, K. Han, S. Zeng, X. Liu, J. Ma, C. Liu, J. Chen, J. Zhang, Ariando, T. V. Venkatesan, S. J. Pennycook, J. M. D. Coey, L. Shen, J. Ma, X. R. Wang, and C.-W. Nan, ACS Appl. Mat. & Interfaces **9**, 44931 (2017).

[15]J. Zhang, X. Chen, Q. Zhang, F. Han, J. Zhang, H. Zhang, H. Zhang, H. Huang, S. Qi, X. Yan, L. Gu, Y. Chen, F. Hu, S. Yan, B. Liu, B. Shen, and J. Sun, ACS Applied Materials & Interfaces **10**, 40951 (2018).

[16]M. Huijben, L. W. Martin, Y.-H. Chu, M. B. Holcomb, P. Yu, G. Rijnders, D. H. A. Blank, and R. Ramesh, Phys. Rev. B **78**, 94413 (2008).

[17]R. Peng, H. C. Xu, M. Xia, J. F. Zhao, X. Xie, D. F. Xu, B. P. Xie, and D. L. Feng, Applied Physics Letters **104**, 081606 (2014).

[18]S. Koohfar, A. S. Disa, M. S. Marshall, F. J. Walker, C. H. Ahn, and D. P. Kumah, Physical Review B **96**, 24108 (2017).

[19]H. Boschker, J. Verbeeck, R. Egoavil, S. Bals, G. van Tendeloo, M. Huijben, E. P. Houwman, G. Koster, D. H. Blank, and G. Rijnders, Adv. Funct. Mater. **22**, 2235 (2012).

[20]J. A. Mundy, Y. Hikita, T. Hidaka, T. Yajima, T. Higuchi, H. Y. Hwang, D. A. Muller, and L. F. Kourkoutis, Nature Communications **5**, 3464 (2014).

[21]Z. Li, M. Bosman, Z. Yang, P. Ren, L. Wang, L. Cao, X. Yu, C. Ke, M. B. Breese, A. Rusydi, W. Zhu, Z. Dong, and Y. L. Foo, Advanced Functional Materials **22**, 4312 (2012).

[22]L. Jin, C.-L. Jia, I. Lindfors-Vrejoiu, X. Zhong, H. Du, and R. E. Dunin-Borkowski, Advanced Materials Interfaces **3**, 1600414 (2016).

ACCEPTED MANUSCRIPT

PLEASE CITE THIS ARTICLE AS DOI: 10.1063/5.0033236

Journal of Applied Physics

AIP Publishing

[23]A. Tebano, C. Aruta, S. Sanna, P. G. Medaglia, G. Balestrino, A. A. Sidorenko, R. De Renzi, G. Ghiringhelli, L. Braicovich, V. Bisogni, and N. B. Brookes, Physical Review Letters **100**, 137401 (2008).

[24]M. Huijben, G. Koster, Z. Liao, and G. Rijnders, Applied Physics Reviews **4**, 041103 (2017).

[25]D. Yi, N. Lu, X. Chen, S. Shen, and P. Yu, Journal of Physics: Condensed Matter **29**, 443004 (2017).

[26]A. Bhattacharya and S. J. May, Annu. Rev. Mater. Res. **44**, 65 (2014).

[27]E. J. Moon, Q. He, S. Ghosh, B. J. Kirby, S. T. Pantelides, A. Y. Borisevich, and S. J. May, Phys. Rev. Lett. **119**, 197204 (2017).

[28]M. Ziese, F. Bern, E. Pippel, D. Hesse, and I. Vrejoiu, Nano Letters **12**, 4276 (2012).

[29]S. Koohfar, A. B. Georgescu, I. Hallsteinsen, R. Sachan, M. A. Roldan, E. Arenholz, and D. P. Kumah, Phys. Rev. B **101**, 064420 (2020).

[30]R. Olmos, H. Iturriaga, D. S. Blazer, S. Koohfar, K. Gandha, I. C. Nlebedim, D. P. Kumah, and S. R. Singamaneni, AIP Advances **10**, 015001 (2020).

[31]A. N. Penn, S. Koohfar, D. P. Kumah, and J. M. LeBeau, AIP Advances **10**, 045113 (2020).

[32]E. Gommert, H. Cerva, J. Wecker, and K. Samwer, Journal of Applied Physics **85**, 5417 (1999).

[33]M.-J. Casanove, C. Roucau, P. Baules, J. Majimel, J.-C. Ousset, D. Magnoux, and J. F. Bobo, Applied Surface Science **188**, 19 (2002).

[34]R. P. Borges, W. Guichard, J. G. Lunney, J. M. D. Coey, and F. Ott, J. Appl. Phys. **89**, 3868 (2001).

[35]C. M. Schleputz, R. Herger, P. R. Willmott, B. D. Patterson, O. Bunk, C. Bronnimann, B. Henrich, G. Hulsen, and E. F. Eikenberry, Acta Cryst. A **61**, 418 (2005).

[36]J. Floro, S. Hearne, J. Hunter, P. Kotula, E. Chason, S. Seel, and C. Thompson, Journal of Applied Physics **89**, 4886 (2001).

[37]M. Bjorck and G. Andersson, J. of Appl. Cryst. **40**, 1174 (2007).

[38]O. Lebedev, J. Verbeeck, G. Van Tendeloo, C. Dubourdieu, M. Rosina, and P. Chaudouet, J. Appl. Phys. **94**, 7646 (2003).

[39]M. Johnson, P. Bloemen, F. Den Broeder, and J. De Vries, Reports on Progress in Physics **59**, 1409 (1996).

ACCEPTED MANUSCRIPT

Journal of Applied Physics

PLEASE CITE THIS ARTICLE AS DOI: 10.1063/5.0033236

[40]D. Yi, C. L. Flint, P. P. Balakrishnan, K. Mahalingam, B. Urwin, A. Vailionis, A. T. N'Diaye, P. Shafer, E. Arenholz, Y. Choi, K. H. Stone, J.-H. Chu, B. M. Howe, J. Liu, I. R. Fisher, and Y. Suzuki, Physical Review Letters **119**, 077201 (2017).

[41]Y. Suzuki, H. Hwang, S.-W. Cheong, T. Siegrist, R. Van Dover, A. Asamitsu, and Y. Tokura, Journal of Applied Physics **83**, 7064 (1998).

[42]D. Pesquera, G. Herranz, A. Barla, E. Pellegrin, F. Bondino, E. Magnano, F. Sánchez, and J. Fontcuberta, Nat. Comm. **3**, 1189 (2012).

AIP Publishing

Journal of Applied Physics

ACCEPTED MANUSCRIPT

PLEASE CITE THIS ARTICLE AS DOI: 10.1063/5.0033236

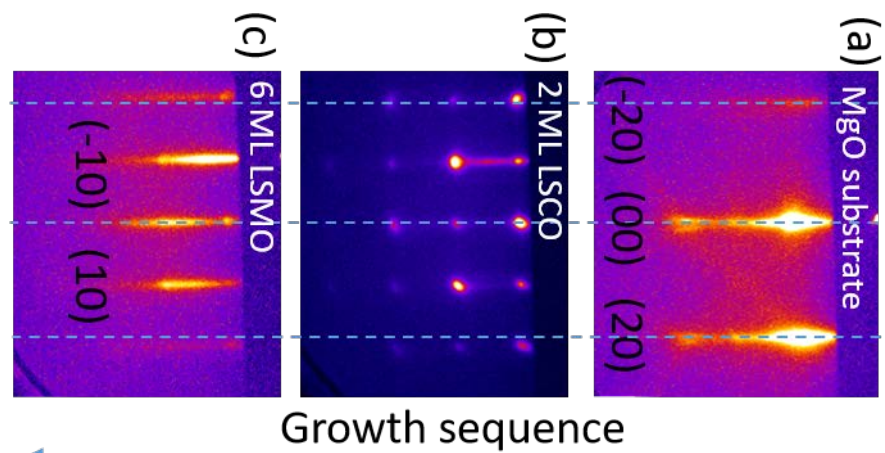

ACCEPTED MANUSCRIPT

PLEASE CITE THIS ARTICLE AS DOI: 10.1063/5.0033236

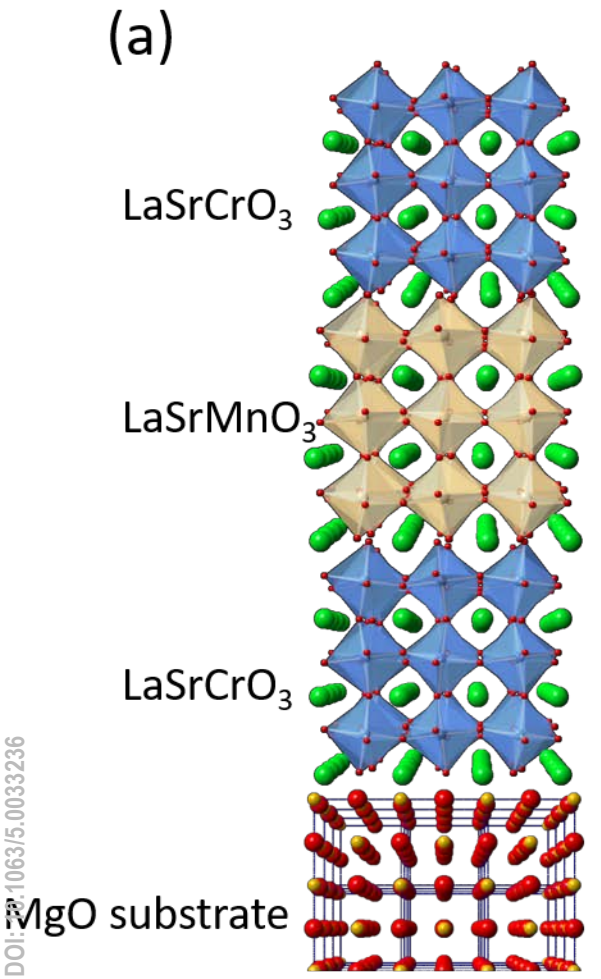

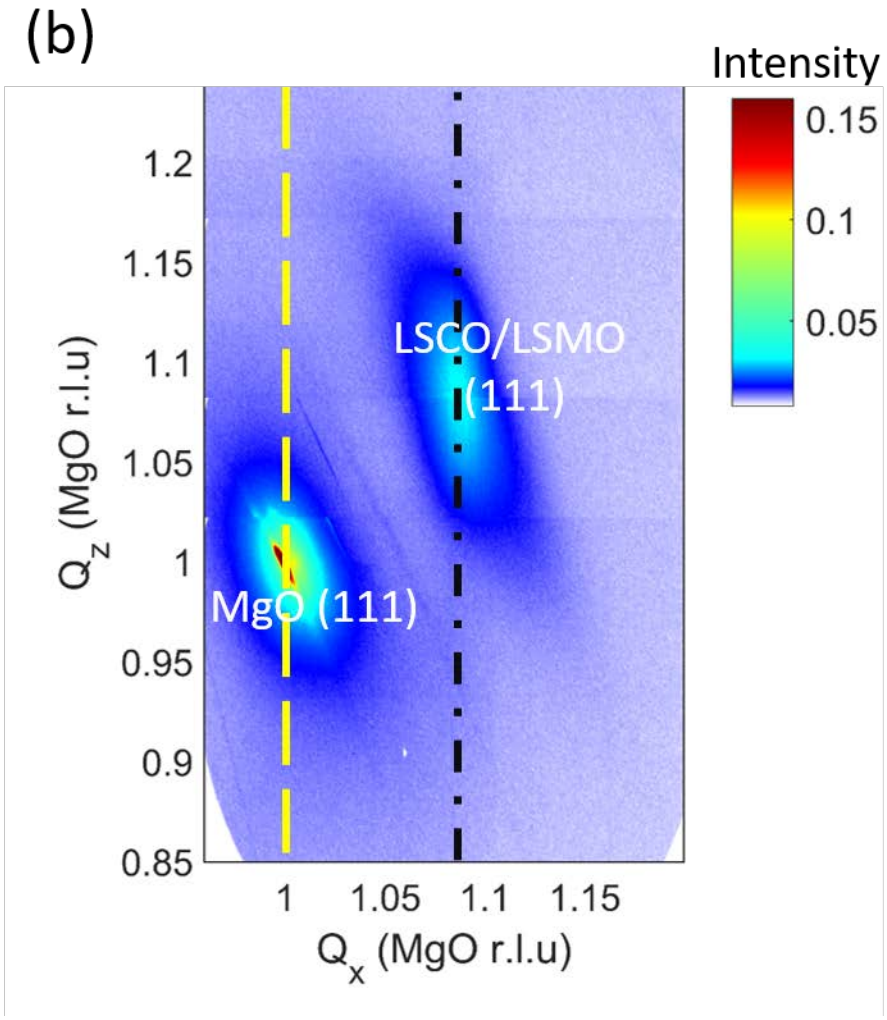

Journal of Applied Physics

AIP Publishing

ACCEPTED MANUSCRIPT

Journal of Applied Physics

AIP Publishing

PLEASE CITE THIS ARTICLE AS DOI: 10.1063/5.0033236

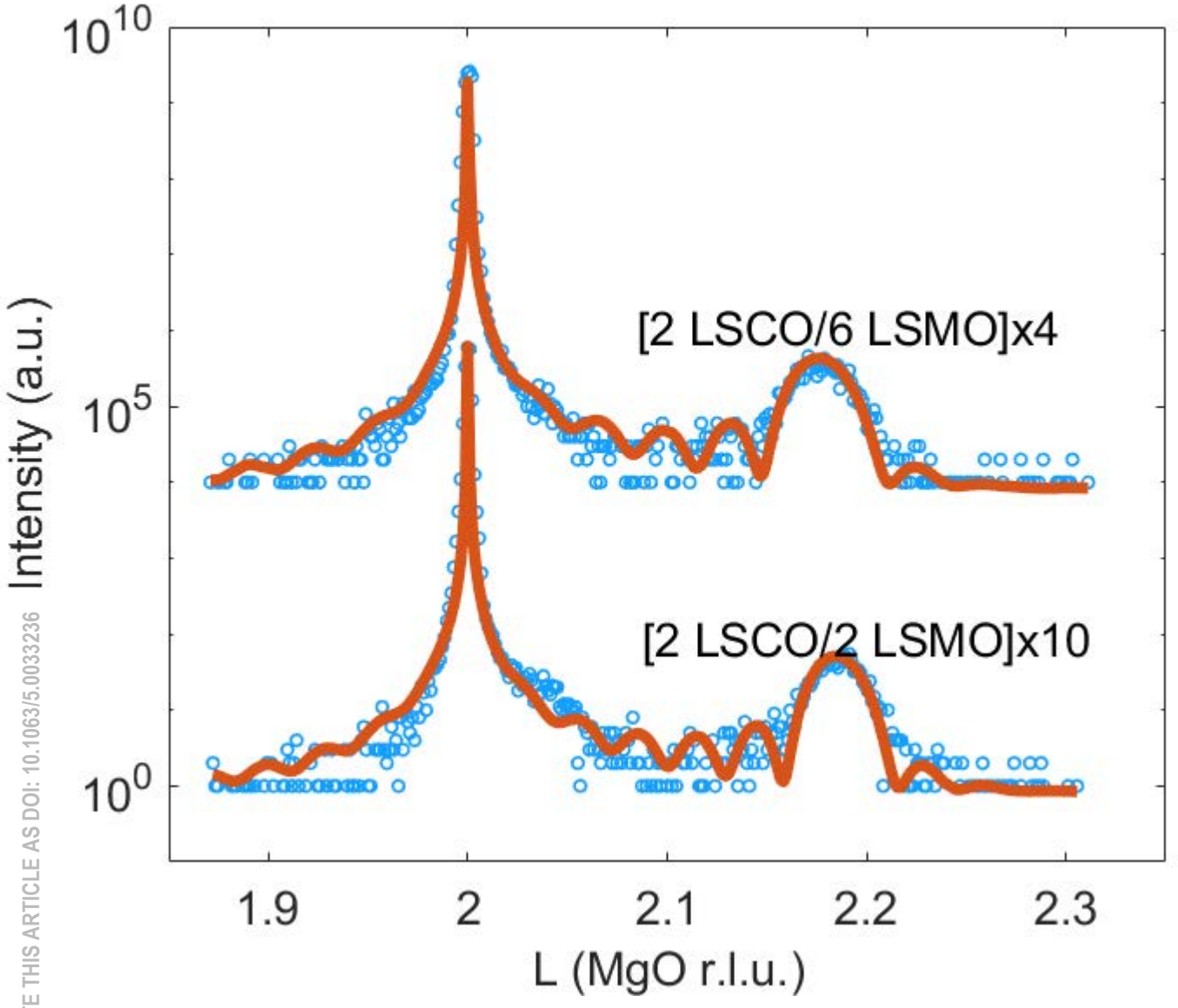

ACCEPTED MANUSCRIPT

PLEASE CITE THIS ARTICLE AS DOI: 10.1063/5.0033236

Journal of Applied Physics

AIP Publishing

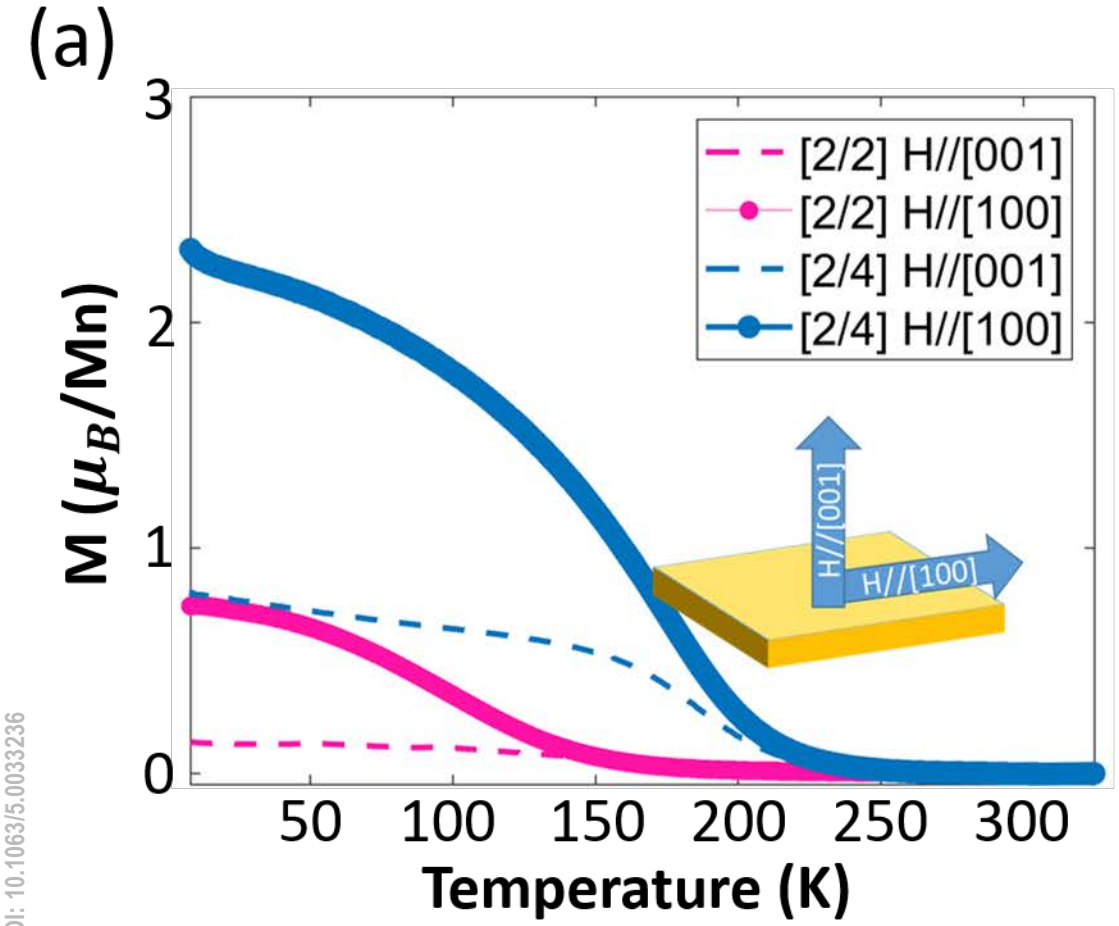

ACCEPTED MANUSCRIPT

PLEASE CITE THIS ARTICLE AS DOI: 10.1063/5.0033236

Journal of Applied Physics

AIP Publishing